Abstracta

Ano XXVIII - N. 05

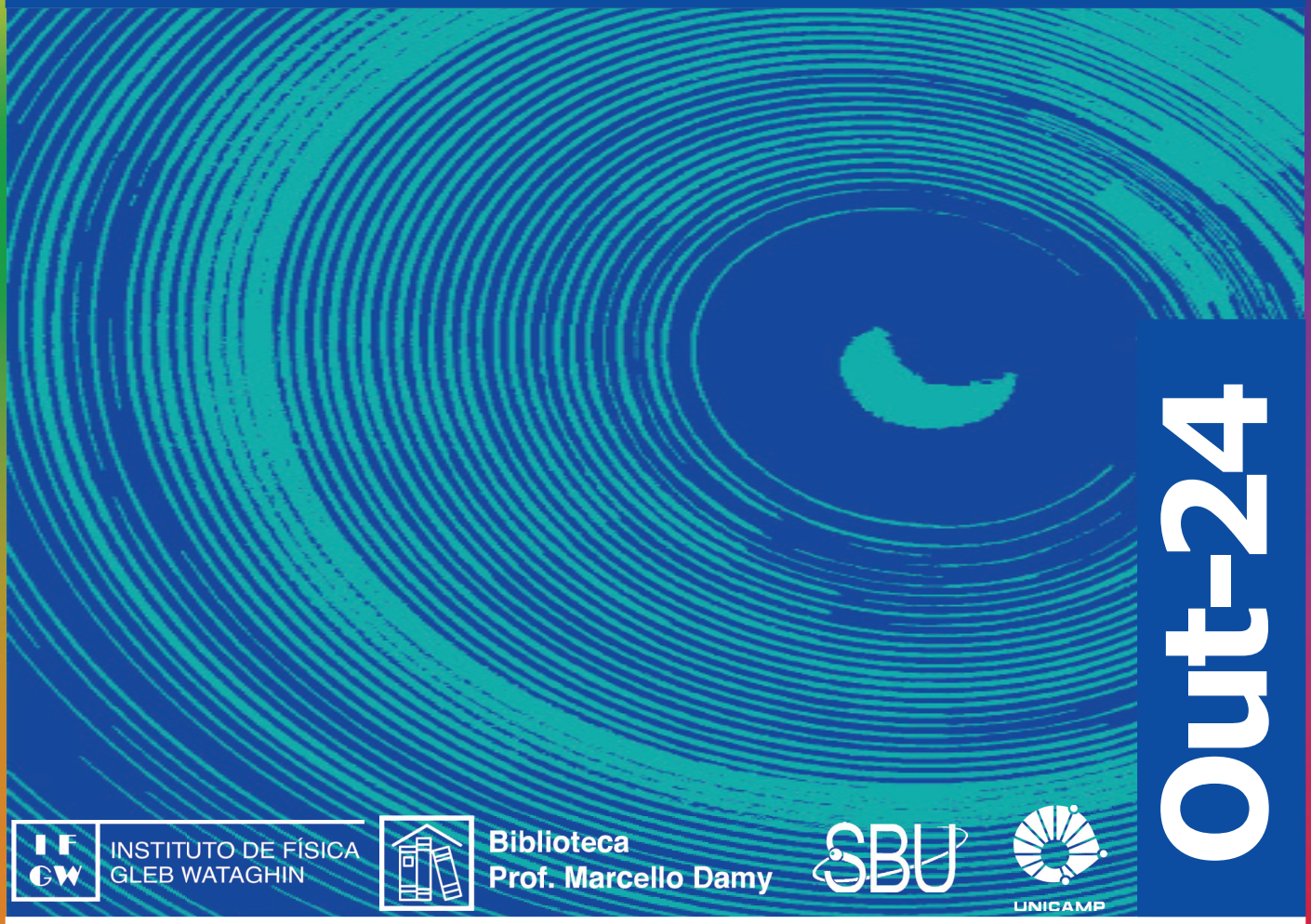

Artigos publicados

[P160-2024] "2D Phase Formation on 3D Perovskite: Insights from Molecular Stiffness"

Scalon, L.; **Nogueira, C. A.*;** Fonseca, A. F. V.; Marchezi, P. E.; Moral, R. F.; Grancini, G.; Kodalle, T.; Sutter-Fella, C. M.; Oliveira, C. C.; **Zagonel, L. F.***; Nogueira, A. F.

Several studies have demonstrated that low-dimensional structures (e.g., two-dimensional (2D)) associated with three--dimensional (3D) perovskite films enhance the efficiency and stability of perovskite solar cells. Here, we aim to track the formation sites of the 2D phase on top of the 3D perovskite and to establish correlations between molecular stiffness and steric hindrance of the organic cations and their influence on the formation and crystallization of 2D/3D. Using cathodoluminescence combined with a scanning electron microscopy technique, we verified that the formation of the 2D phase occurs preferentially on the grain boundaries of the 3D perovskite. This helps explain some passivation mechanisms conferred by the 2D phase on 3D perovskite films. Furthermore, by employing in situ grazing-incidence wide-angle X-ray scattering, we monitored the formation and crystallization of the 2D/3D perovskite using three cations with varying molecular stiffness. In this series of molecules, the formation and crystallization of the 2D phase are found to be dependent on both steric hindrance around the ammonium group and molecular stiffness. Finally, we employed a 2D/3D perovskite heterointerface in a solar cell. The presence of the 2D phase, particularly those formed from flexible cations, resulted in a maximum power conversion efficiency of 21.5%. This study provides insight into critical aspects related to how bulky organic cations' stiffness and steric hindrance influence the formation, crystallization, and distribution of 2D perovskite phases.

ACS APPLIED MATERIALS & INTERFACES 16[38], 51727-51737, 2024. DOI: 10.1021/acsami.4c11394 Early Access Date: SEP 2024

[P161-2024] "A Teleoperated Robotic System with Haptic Feedback for Soft Tissue Incision"

García-Cárdenas, F.; **Fabian, J.***; Ramos, O. E.; Canahuire, R.

The teleoperation of robotic manipulators allows extending the capabilities of human operators to work in different scales and distances to improve the efficiency of tasks that require high precision and repeatability. However, the lack of kinesthetics makes teleoperation difficult under diminished visibility or during palpation tasks despite visual and auditory feedback. This work presents the design and implementation of a haptic teleoperation system based on a master-slave hybrid control scheme. The robotic system uses a haptic device and a joystick to map the desired pose of the robot, while a force sensor located in the end-effector provides stiffness perception. The implemented control algorithm employs a weighted quadratic program to compute the inverse kinematics at different scales, allowing the system to operate over delicate and uneven surfaces, such as those found in surgical incisions. Finally, experimental results are shown, where the performance of the haptic system in cutting porcine tissue and manipulation tasks inside the free workspace are discussed.

JOURNAL OF CONTROL AUTOMATION AND ELECTRICAL SYSTEMS 35[5], 870-883, 2024. DOI: 10.1007/s40313-024-01117-6

[P162-2024] "Assortativity in sympatric speciation and species classification"

Lizarraga, J. U. F.*; Marquitti, F. M. D.*; Aguiar, M. A. M. de*

We investigate the role of assortative mating in speciation using the sympatric model of Derrida and Higgs. The model explores the idea that genetic differences create incompatibilities between individuals, preventing mating if the number of such differences is too large. Speciation, however, only happens in this mating system if the number of genes is large. Here we show that speciation with small genome sizes can occur if assortative mating is introduced. In our model individuals are represented by three chromosomes: one responsible for reproductive compatibility, one for coding the trait on which assortativity will operate, and a neutral chromosome. Reproduction is possible if individuals are genetically similar with respect to the first chromosome, but among these compatible mating partners, the one with the most similar trait coded by the second chromosome is selected. We show that this type of assortativity facilitates speciation, which can happen with a small number of genes in the first chromosome. Species, classified according to reproductive isolation, dictated by the first chromosome, can display different traits values, as measured by the second and the third chromosomes. Therefore, species can also be identified based on similarity of the neutral trait, which works as a proxy for reproductive isolation.

PHYSICA A-STATISTICAL MECHANICS AND ITS APPLICATIONS 653, 130111, 2024. DOI: 10.1016/j.physa.2024.130111

[P163-2024] "Atomic Structure and 3D Shape of a Multibranched Plasmonic Nanostar from a Single Spatially Resolved Electron Diffraction Map"

Corrêa, L. M.*; Fairclough, S. M.; Scher, K. M. R; Atta, S.; Santos, D. P. dos; Ducati, C.; Fabris, L.; **Ugarte, D.***

Despite the interest in improving the sensitivity of optical sensors using plasmonic nanoparticles (NPs) (rods, wires, and stars), the full structural characterization of complex shape nanostructures is challenging. Here, we derive from a single scanning transmission electron microscope diffraction map (4D-STEM) a detailed determination of both the 3D shape and atomic arrangement of an individual 6-branched AuAg nanostar (NS) with high-aspect-ratio legs. The NS core displays an icosahedral structure, and legs are decahedral rods attached along the 5-fold axes at the core apexes. The NS legs show an anomalous anisotropic spatial distribution (all close to a plane) due to an interplay between the icosahedral symmetry and the unzipping of the surfactant layer on the core. The results significantly improve our understanding of the star growth mechanism. This low dose diffraction mapping is promising for the atomic structure study of individual multidomain, multibranched, or multiphase NPs, even when constituted of beam-sensitive materials.

ACS NANO 18[39], 26655-26665, 2024. DOI: 10.1021/acsnano.4c05201

[P164-2024] "Band gap opening in Bernal bilayer graphene under applied electric field calculated by DFT"

Silva, D. H. S.*

This paper proposes the induction and further analysis of band gap opening in Bernal bilayer graphene based on Density Functional Theory (DFT). By simulating a sawtooth-like potential configured so that the electric field (the slope) ranges from 1 V/nm to 10 V/nm, it was found that the band gap reached approximately 325 meV, where it saturated. Although the band gap was consistently direct, it was observed that as the applied electric field increased, the band gap shifted from the high-symmetry K point to other points.

PHYSICA B-CONDENSED MATTER 694, 416398, 2024. DOI: 10.1016/j.physb.2024.416398

[P165-2024] "C-Arapuca: An Innovative Device for Detecting Cherenkov Radiation"

Fauth, A. C.*; Machado, A. A.*; Pimentel, V. do L.; **Segreto, E.***

We present the development of a new device, which we named C-Arapuca, capable of detecting photons from Cherenkov radiation produced in water. This device employs the concept of trapping photons within a box that features highly reflective internal walls and contains a few small silicon photomultipliers. We describe how the trapping process is carried out by a dichroic filter and a wavelength shifter bar. Two prototypes of this new photodetector were installed in a tank of ultrapure water, and charge spectra generated by muons from local cosmic radiation were studied. The results obtained confirm the feasibility of using the photon trapping concept for Cherenkov radiation detection in water.

BRAZILIAN JOURNAL OF PHYSICS 54[6], 242, 2024. DOI: 10.1007/s13538-024-01616-6

[P166-2024] "Chaotic dynamics of pulsating spheres orbiting black holes"

Rodrigues, F. de F.*; Mosna, R. A.*; Vieira, R. S. S.

We study the chaotic dynamics of spinless extended bodies in a wide class of spherically symmetric spacetimes, which encompasses black-hole scenarios in many modified theories of gravity. We show that a spherically symmetric pulsating ball may have chaotic motion in this class of spacetimes. The cases of the Reissner-Nordstr & ouml;m and Ay & oacute;n-Beato-Garc & iacute;a black holes are analyzed in detail. The equations of motion for the extended bodies are obtained according to Dixon's formalism, up to quadrupole order. Then, we use Melnikov's method to show the presence of homoclinic intersections, which imply chaotic behavior, as a consequence of our assumption that the test body has an oscillating radius.

GENERAL RELATIVITY AND GRAVITATION 56[10], 112, 2024. DOI: 10.1007/s10714-024-03300-1

[P167-2024] "Combining physics-informed neural networks with the freezing mechanism for general Hamiltonian learning"

Castelano, L. K.; Cunha, I.; Luiz, F. S.; Napolitano, R. de J.; Prado, M. V. de S.; **Fanchini, F. F.***

The precision required to characterize a Hamiltonian is central to developing advantageous quantum computers, providing powerful advances in quantum sensing and crosstalk mitigation. Traditional methods to determine a Hamiltonian are difficult due to the intricacies of quantum systems, involving numbers of equations and parameters that grow exponentially with the number of qubits. To mitigate these shortcomings, in this paper, we introduce an innovative and effective procedure integrating a physics-informed neural network (PINN) with a freezing mechanism to learn the Hamiltonian parameters efficiently. Although PINN and experimental data alone would become impractical as N increases, the mechanism we introduce freezes the interactions of most of the qubits, leaving just a qubit subsystem to be analyzed by the PINN method. Determination of all physical parameters is accomplished by analyzing the system by parts until completion. We validated the efficacy of our method using simulation data obtained from the IBM quantum computer to obtain the training data and we found that a PINN can learn the two-qubit parameters with high accuracy, achieving a median error of less than 0.1% for systems of up to four qubits. We have successfully combined the PINN analysis of two qubits with the freezing mechanism in the case of a four-qubit system.

PHYSICAL REVIEW A 110[3], 032607, 2024. DOI: 10.1103/PhysRevA.110.032607

[P168-2024 "Dark energy survey year 3 results: miscentring calibration and X-ray-richness scaling relations in redMaPPer clusters"

Kelly, P. M.; Jobel, J.; Eiger, O.; **Sahlen, M.***; et al..
DES Collaboration

We use Dark Energy Survey Year 3 (DES Y3) clusters with archival XMM-Newton and Chandra X-ray data to assess the centring performance of the redMaPPer cluster finder and to measure key richness observable scaling relations. We find that 10-20 per cent of redMaPPer clusters are miscentred, both when comparing to the X-ray peak position and to the visually identified central cluster galaxy. We find no significant difference in miscentring in bins of low versus high richness or redshift. The dominant reasons for miscentring include masked or missing data and the presence of other bright galaxies in the cluster. For half of the miscentred clusters, the correct central was one of the possible centrals identified by redMaPPer, while for similar to 40 per cent of miscentred clusters, the correct central is not a redMaPPer member mostly due to masking. Additionally, we fit scaling relations of X-ray temperature and luminosity with richness. We find a TX-lambda scatter of 0.21 +/- 0.01. While the scatter in TX-lambda is consistent in redshift bins, we find modestly different slopes, with high-redshift clusters displaying a somewhat shallower relation. Splitting based on richness, we find a marginally larger scatter for our lowest richness bin, 20 < lambda < 40. We note that the robustness of the scaling relations at lower richnesses is limited by the unknown selection function, but at lambda > 75, we detect nearly all of the clusters falling within existing X-ray pointings. The X-ray properties of detected, serendipitous clusters are generally consistent with those of targeted clusters.

MONTHLY NOTICES OF THE ROYAL ASTRONOMICAL SOCIETY 533[1], 572-588, DOI: 10.1093/mnras/stae1786

[P169-2024] "Drop-Weight Impact Resistance of 3D-Printed Complex Zeolite-Inspired Structures"

Ambekar, R. S.; Oliveira, E. F.; Pugazhenthi, P.; Singh, S.; Mahapatra, D. R.; **Galvao, D. S.***; Tiwary, C. S.

Ballistic resistance architectures have crucial importance in the defense and aerospace industries. The researchers are constantly excited to explore lightweight, complex architectures for higher mechanical energy absorption. The complexity of the design is restricted due to a lack of advanced manufacturing techniques. However, additive manufacturing (AM)/3D printing facilitates sustainability, excellent design flexibility, and automation. The zeolite-inspired 3D printed structures are designed and developed to study deformation under low-velocity drop impact. The present work has the comparison of the specific energy absorption of different types of zeolite-inspired structures. It also has the effect of velocity on impact depth at multiscale using molecular dynamics (theoretical) and computer tomography (experimental). Zeolite-templated porous structures are designed and developed to understand the deformation behavior under low-velocity ballistic impact. Advanced manufacturing techniques are utilized to fabricate complex structures, and computer tomography is employed to study the internal deformation mechanism. To complement results, Molecular dynamics simulations are carried out in order to qualitatively compare the deformation behavior of the structures.

ADVANCED ENGINEERING MATERIALS, 2024. DOI: 10.1002/adem.202400035

[P170-2024] "Effects of Ti and Y on resistance to corrosion in Fe-Cr-X Alloys"

Jesus, T. J. M.; Souza, S. A.; Barreto, B. C.; Santana, A. I. C.; **Landers, R.***; Caram, R.; Silva, M. S. C.; Rodrigues, J. F. Q.; Afonso, C. R. M.; Macedo, M. C. S. S.

The effect of Ti and Y on the corrosion behavior of the FeCr alloy was investigated in a 3.5% NaCl solution. Ti was found to inhibit the formation of the a phase, significantly reducing the presence of pitting in the material. In addition, Ti acted indirectly on the oxide layer, increasing the concentrations of Cr and Fe, consequently generating a probable enrichment of Cr2O3 and FeOOH, which enabled the formation of a more stable passive film resistant to attack by chloride ions. On the other hand, Y caused the precipitation of a phase identified as Fe17Y2, which was accompanied by an elongated a phase, both located at the grain boundaries, besides the formation of Cr23C6 and Y2O3. Its addition resulted in an improvement in the corrosion resistance of the FeCr alloy by reducing the precipitation of the a phase. However, its effect was much less important than that of Ti, since the results showed that the FeCrY alloy was still highly susceptible to localized forms of corrosion.

JOURNAL OF MATERIALS RESEARCH AND TECHNOLOGY-JMR&T 33, 1600-1622, 2024. DOI: 10.1016/j.jmrt.2024.09.166

[P171-2024] "Emergence of Long-Range Angular Correlations in Low-Multiplicity Proton-Proton Collisions"

Acharya, S.; Adamova, D.; Rinella, G. A.; **Chinellato, D. D.*; Guardiano, G. G.*; Liveraro, G. S. S.*; Takahashi, J.***; et al. ALICE Collaboration

This Letter presents the measurement of near-side associated per-trigger yields, denoted ridge yields, from the analysis of angular correlations of charged hadrons in proton- proton collisions at root s=13 TeV. Long-range ridge yields are extracted for pairs of charged particles with a pseudorapidity difference of 1.4 < Delta eta < 1.8 and a transverse momentum of 1 < pr < 2 GeV/c, as a function of the charged-particle multiplicity measured at midrapidity. This Letter extends the measurements of the ridge yield to the low multiplicity region, where in hadronic collisions it is typically conjectured that a strongly interacting medium is unlikely to be formed. The precision of the new low multiplicity results allows for the first direct quantitative comparison with the results obtained in ethorne- collisions at root s=91 GeV and root s 183-209 GeV, where initial-state effects such as preequilibrium dynamics and collision geometry are not expected to play a role. In the multiplicity range 8.<= N(eh <=)24 where the ethorne- results have good precision, the measured ridge yields in pp collisions are substantially larger than the limits set in ethorneannihilations. Consequently, the findings presented in this Letter suggest that the processes involved in ethorne- annihilations do not contribute significantly to the emergence of long-range correlations in pp collisions.

PHYSICAL REVIEW LETTERS 132[17], 172302, 2024. DOI: 10.1103/PhysRevLett.132.172302

[P172-2024] "Enantioselective optical forces and size-dependent sorting of single chiral particles using vortex beams"

Ali, R.*; Pinheiro, F. A.; Dutra, R. S.; **Alegre, T. P. M.*; Wiederhecker, G. S.***

We put forward an approach to manipulate and enantioselect chiral microspheres using vortex beams that encode topological charges. Vortex beams with different topological charges transfer angular momentum to chiral particles with opposite handedness in a different way. This process also depends on the incident polarization, in a rich interplay that ultimately leads to enantioselective optical forces acting on single chiral particles with selected, arbitrary sizes. Besides this scheme also depends on the order of the topological charge, which can also be controlled experimentally. The resulting enantioselective optical forces are up to two orders of magnitude larger than the existing chiral resolution methods based on optical forces, further demonstrating the unique functionalities and applicability of the method.

PHYSICAL REVIEW B 110[11], 115412, 2024. DOI: 10.1103/PhysRevB.110.115412

[P173-2024] "Enhancing the Goos-Hänchen and spin-Hall shifts in planar and spherical structures through complex--frequency excitations"

Ali, R.*; Alegre, T. P. M.*; Wiederhecker, G. S.*

The scattering of an electromagnetic field oscillating in a complex-frequency plane is known to capture and release energy within a lossless cavity, yielding virtual loss and virtual gain, respectively. In this context, we use electromagnetic with complex frequency to optimize both the longitudinal beam shifts (Goos-H & auml;nchen shift) and transversal beam shifts (spin-Hall shift) in the transmitted field through the slab and scattered field by the sphere. The results demonstrate a significantly large gradient in the transmission amplitude due to the occurrence of scattering poles in the lower half plane of the complex frequency. In addition, the complex frequency allows the suppression of both forward and backward scattering by the spherical cavity. Consequently, the scattered plane undergoes a substantial shift, leading to an enhanced Goos-H & auml;nchen shift and spin-Hall shift in both planar and spherical cavities. Importantly, this scheme relies on the incident-beam profile without the need for engineering materials parameters of the cavity. As a result, it surpasses previous methods that rely on materials engineering to optimize the beam shifts. To underscore the broad applicability and versatility of the current formalism, we have chosen to implement it using the commercial software COMSOL and found perfect agreement with the analytical results.

PHYSICAL REVIEW B 110[8], 085403, 2024. DOI: 10.1103/PhysRevB.110.085403

[P174-2024] "Generating proton-disordered ice configurations using orientational simulated annealing"

Cândido, V. F.*; Veiga, R. G. de A.; **Koning, M. de***

We examine an algorithm for the creation of proton-disordered ice cells based on a simulated-annealing (SA) scheme for molecular orientations. Application to defect-free ice Ih, a clathrate-hydrate structure, and a random polycrystalline ice Ih sample demonstrates the SA technique to be effective, attaining maximum HB connectivity using relatively short cooling simulations, thus serving as an alternative method for those cases in which the application of topology-based methods is inhibited.

JOURNAL OF CHEMICAL PHYSICS 161[6], 066101, 2024. DOI: 10.1063/5.0220111

[P175-2024] "Hybrid Paper/Polyester-Based Laser-Induced Graphene Electrodes for Electrochemical Detection of Tadalafil"

Souza, S. G. G.; Silva-Neto, H. A.; Rocha, D. S.; **Siervo, A. de***; Paixao, T. R. L. C.; Coltro, W. K. T.

Here, we describe for the first time the fabrication of laser--induced graphene (LIG) electrodes on a hybrid substrate composed of sandpaper and polyester. As a proof of concept, the proposed device was used as a voltammetric sensor for tadalafil (TAD) quantification in authentic tablet samples. The electrochemical TAD sensing based on differential pulse voltammetry (DPV) revealed a linear behavior in the concentration range from 25 to 250 mu mol L-1(R-2=0.99), a limit of detection of similar to 9.6 mu mol L-1, sensitivity of similar to 0.0048 mu A(mu mol L-1)(-1) and acceptable reproducibility values (RSD <= 5.8 %). The DPV responses involving the standard addition method in pharmaceutical samples presented recovery results of TAD ranging from 93 to 108 %. Also, the proposed analytical method offered a suitable green analytical chemistry profile. We successfully demonstrated the fabrication of graphene-like sites and nanoparticles composed of alumina upon a hybrid substrate.

ANALYSIS & SENSING, e202400016, 2024. DOI: 10.1002/anse.202400016

[P176-2024] "Indirect Surface-Enhanced Raman Scattering Sensor for Direct Detection of Gaseous Elemental Mercury"

Santos, D. A. L.; Barros, A. de; Santos, D. P. dos; Pereira, G. C.; **Shimizu, F. M.***; Fostier, A. H.; Sigoli, F. A.; Mazali, I. O.

Gaseous elemental mercury (GEM & horbar;Hg-(g)(0)) is a highly toxic global pollutant with environmental and human health effect concerns. Monitoring the GEM released in gold mining operation regions is extremely necessary. Herein, we develop an indirect surface-enhanced Raman scattering (SERS)-miniaturized sensor for the direct detection of Hg--(g)(0) using gold nanorods (AuNRs) and rhodamine 6G as a probe molecule. SERS spectra show a suppressed signal after exposure to Hg-(g)(0) in different concentrations caused by the morphologic transition of the nanorods to spheres. Discrete dipole approximation (DDA) and density functional theory (DFT) simulations reveal that the energetic phenomena involved during the Au-Hg amalgam formation process can lead to drastic changes in the AuNR's plasmonic characteristic, suppressing the SERS signal. This effect is the key to achieving the high performance to detect Hg-(g)(0) until 0.08 mu g. Additionally, the SEM-EDS results confirmed the AuNR's morphological changes after exposure to Hg-(g)(0), and principal component analysis and root-mean-square error reveal the high sensitivity, mainly for the lower amount of Hg-(g)(0) (0.08-1.02 mu g), corroborating the DDA and DFT simulations whose Au-Hg alloy formation on the AuNR's surface is energetically more favorable, occurring more quickly and efficiently than the diffusion process. Moreover, these results show nanorod structures are more efficient than spherical ones.

ACS APPLIED NANO MATERIALS 7[15], 17251-17261, 2024. DOI: 10.1021/acsanm.4c01233

[P177-2024] "Influence of anions on the structural and catalytic properties of CTA-MCM-41"

Assis, F. M. de; Ribeiro, M. E.; Zapelini, I. W.; **Landers, R.***; Cardoso, D.

CTA-MCM-41 - Mobil Composition of Matter 41 with cetyltrimethylammonium cations (CTA(+)) - is a hybrid silica known for its high basic catalytic activity due to anionic silanolate sites (Si-O-) that are bound to CTA(+). The synthesis of this material depends on the properties of CTA(+) micelles in aqueous dispersion which, in turn, depend on the surrounding anions. Thus, this study investigated different types and amounts of anions in the synthesis of CTA-MCM-41. Chloride (Cl-), bromide (Br-), iodide (I-), nitrate (NO3-) and hydroxide (OH-) anions in sodium form were added to the synthesis mixture, and the obtained silicas were tested in the transesterification reaction. It is hereby presented a comprehensive study on how micelles-anion interfaces play a key role in the synthesis of this important hybrid silica catalyst, and it was possible to synthesize a more active basic catalyst than the conventional CTA-MCM-41, just by exploring such surface chemistry effects. Three significant features are highlighted: (1) improved catalytic activity of CTA-MCM-41 applied in transesterification; (2) Synthesis of CTA-MCM-41 with higher retention of cations per silica and higher amount of silanolate basic sites; (3) deepening knowledge of the synthesis mechanism of materials from the MCM-41 family. The effects are more pronounced in the order I- > NO3- > Cl-, in accordance with the Hofmeister ion series. Hydroxide anions, however, led to the greatest increase in the number of sites and basic catalytic activity (up to 52.4 %). These results reinforce the validity of the {S+, X-, I-} (S: surfactant; X: anion; I: silica) silica formation mechanism and reveal a synthesis with hydroxide anions that produces a catalyst more active than conventional CTA-MCM-41.

COLLOIDS AND SURFACES A-PHYSICOCHEMICAL AND ENGINEERING ASPECTS 701, 134850, 2024. DOI: 10.1016/j.colsurfa.2024.134850

[P178-2024] "Innovative proposal for N2 2 capturing in Liquid Argon using the Li-FAU molecular Sieve"

Cardoso, D.; **Segreto, E.*; Freitas, G. S.*; Caffer, A. M.*; Souza, J. C.*; Christovam, D. S.*; Wiederhecker, G.*; Santos, C. R. A. de*; Correia, D.*; Frandini, H.*; Demolin, F.*; Alegre, T. P. M.*; Adriano, C.*; Machado, A. A.*; Pagliuso, P. G.***; et al.

In this work, we unveil the potential of nitrogen (N-2) adsorption from Liquid Argon (LAr) through the molecular sieves (zeolites) Li-FAU Adsorbents. We report detailed studies about N-2 gas adsorption at T = 89 K using a commercial Micromeritics ASAP-2420 equipment and N-2 purification from LAr using the Purification Cryostat (PuLArC) at IFGW/Unicamp. We argue that the N-2 adsorption by the Li-FAU is possible thanks to the stronger interaction of N-2 with the lithium cations present in zeolite Li-FAU. In fact, the experiments performed in PuLArC have unequivocally shown that the Li-FAU adsorbent was capable of capturing N-2, reducing a N-2 contamination of 20-50 ppm to 0.1-1.0 ppm in 1-2 hours of circulation time in LAr for several runs. This result demonstrated the great potential of the Li-FAU adsorbent for N-2 capturing in LAr and invoke further tests of this material in larger scale LAr cryostats in order to confirm the innovative proposal of using the Li-FAU molecular sieve in replacement of Molecular Sieve 4A, currently used in LAr cryostats for neutrino experiments.

JOURNAL OF INSTRUMENTATION 19[8], C08001, 2024. DOI: 10.1088/1748-0221/19/08/C08001

[P179-2024] "Irida-graphene phonon thermal transport via non-equilibrium molecular dynamics simulations"

Felix, I. M.; Tromer, R. M.; Machado, L. D.; **Galvao, D. S.***; Ribeiro Jr., L. A.; Pereira, M. L.

Recently, a new 2D carbon allotrope called Irida-Graphene (Irida-G) was proposed, and its reliable stability has been previously predicted. Irida-G is a flat sheet topologically arranged into 3-6-8 carbon rings exhibiting metallic and non-magnetic properties. In this study, we investigated the thermal transport properties of Irida-G using classical reactive molecular dynamics simulations. The findings indicate that Irida-G has an intrinsic thermal conductivity of approximately 215 W mK(-1) at room temperature, significantly lower than that of pristine graphene.

This decrease is due to characteristic phonon scattering within Irida-G's porous structure. Additionally, the phonon group velocities and vibrational density of states for Irida-G were analyzed, revealing reduced average phonon group velocities compared to graphene. The thermal conductivity of Irida-G is isotropic and shows significant size effects, transitioning from ballistic to diffusive heat transport regimes as the system length increases. These results suggest that while Irida-G has lower thermal conductivity than graphene, it still holds potential for specific thermal management applications, sharing characteristics with other two-dimensional materials.

NANOSCALE 16[35], 2024. DOI: 10.1039/d4nr02669a

[P180-2024] "Kuramoto variables as eigenvalues of unitary matrices"

Novaes, M.*; Aguiar, M. A. M. de*

We generalize the Kuramoto model by interpreting the N variables on the unit circle as eigenvalues of a N-dimensional unitary matrix U in three versions: general unitary, symmetric unitary, and special orthogonal. The time evolution is generated by N2 coupled differential equations for the matrix elements of U, and synchronization happens when U evolves into a multiple of the identity. The Ott-Antonsen ansatz is related to the Poisson kernels that are so useful in quantum transport, and we prove it in the case of identical natural frequencies. When the coupling constant is a matrix, we find some surprising new dynamical behaviors.

PHYSICAL REVIEW E 110[2], 024217, 2024. DOI: 10.1103/PhysRevE.110.024217

[P181-2024] "Length and torsion dependence of thermal conductivity in twisted graphene nanoribbons"

Fonseca, A. F.*; Pereira, L. F. C.

Research on the physical properties of materials at the nanoscale is crucial for the development of breakthrough nanotechnologies. One of the key properties to consider is the ability to conduct heat, i.e., its thermal conductivity. Graphene is a remarkable nanostructure with exceptional physical properties, including one of the highest thermal conductivities (TCs) ever measured. Graphene nanoribbons (GNRs) share most fundamental properties with graphene, with the added benefit of having a controllable electronic bandgap. One method to achieve such control is by twisting the GNR, which can tailor its electronic properties, as well as change their TCs. Here, we revisit the dependence of the TC of twisted GNRs (TGNRs) on the number of applied turns to the GNR by calculating more precise and mathematically well defined geometric parameters related to the TGNR shape, namely, its twist and writhe. We show that the dependence of the TC on twist is not a simple function of the number of turns initially applied to a straight GNR. In fact, we show that the TC of TGNRs requires at least two parameters to be properly described. Our conclusions are supported by atomistic molecular dynamics simulations to obtain the TC of suspended TGNRs prepared under different values of initially applied turns and different sizes of their suspended part. Among possible choices of parameter pairs, we show that TC can be appropriately described by the initial number of turns and the initial twist density of the TGNRs.

PHYSICAL REVIEW MATERIALS 8[8], 084001, 2024. DOI: 10.1103/PhysRevMaterials.8.084001

[P182-2024] "Localized three-photon upconversion enhancement in silver nanowire networks and its effect in thermal sensing"

Martínez, E. D.; **Ferreira, L. H. A. R.*;** Carneiro Neto, A. N.; Brites, C. D. S.; Carlos, L. D.

The quest for enhancing the upconversion luminescence (UCL) efficiency of rare-earth doped materials has been a common target in nanophotonics research. Plasmonic nanoarchitectures have proven potential for amplifying UCL signals, prompting investigations into localized enhancement effects within noble metal nanostructures. In this work we investigate the localized enhancement of UCL in silver nanowire (AgNW) networks coated with upconversion nanoparticles (UCNPs) by employing hyperspectral microscopy to unveil distinctive regions of local enhancement. Our study reveals that three-photon upconversion processes predominantly occur at hot-spots in nanowire junctions, contributing to heightened luminescence intensity on AgNW networks. Intriguingly, our findings demonstrate that enhancement on AgNWs introduces significant artifacts for thermometry based on ratiometric analysis of the emission spectra, resulting in the observation of artificial thermal gradients. To address this challenge, we developed correction methods that were successfully applied to mitigate this effect, enabling the generation of accurate thermal maps and the realization of dynamic thermal measurements. We quantified the distance-dependent enhancement profiles and studied the effect of temperature by exploiting the heat dissipation under varying electrical voltages across the electrically percolated AgNW networks. The observations were confirmed through numerical calculations of the enhancement factor and the energy transfer rates. This comprehensive investigation sheds light on the complex interplay between plasmonic nanostructures, three-photon upconversion processes, and their influence on thermal sensing applications. The presented hyperspectral method not only allows a direct visualization of plasmonic hot-spots but also advances our understanding of localized enhancements. The correction methods applied to analyze the emission spectra also contribute to the refinement of accurate temperature mapping using UCNPs, thereby enhancing the reliability of this thermal sensing technology. Localized enhancement of upconversion luminescence in silver nanowires allows the direct visualization of plasmonic hot-spots; however, the effect on the emission spectra of Er3+ ions must be corrected for accurate ratiometric thermometry analysis.

NANOSCALE, 2024. DOI: 10.1039/d4nr02484b, Early Access Date: SEP 2024

[P183-2024] "Localized-states quantum confinement induced by roughness in CdMnTe/CdTe heterostructures grown on Si(111) substrates"

Rodrigues, L. N.; Inoch, W. F.; **Gomes, M. L. F.*; Couto Jr., O. D. D.***; Archanjo, B. S.; Ferreira, S. O.

This work shows that despite a lattice mismatch of almost 20%, CdMnTe/CdTe/CdMnTe heterostructures grown directly on Si(111) have surprisingly good optical emission properties. The investigated structures were grown by molecular beam epitaxy and characterized by scanning transmission electron microscopy, macro- and micro-photoluminescence. Low temperature macro-photoluminescence experiments indicate three emission bands which depend on the CdTe layer thickness and have different confinement characteristics. Temperature measurements reveal that the lower energy emission band (at 1.48 eV) is associated to defects and bound exciton states, while the main emission at 1.61 eV has a weak 2D character and the higher energy one at 1.71 eV has a well-defined (zero-dimensional, 0D) 0D nature. Micro-photoluminescence measurements show the existence of sharp and strongly circularly polarized (up to 40%) emission lines which can be related to the presence of Mn in the heterostructure. This result opens the possibility of producing photon sources with the typical spin control of the diluted magnetic semiconductors using the low-cost silicon technology.

JOURNAL OF SEMICONDUCTORS 45[9], 092301, 2024. DOI: 10.1088/1674-4926/24030022

[P184-2024] "Measurement of the fraction of jet longitudinal momentum carried by Λc+ baryons in pp collisions"

Acharya, S.; Adamova, D.; Adler, A.; **Chinellato, D. D.*; Guardiano, G. G.*; Jahnke, C.*; Takahashi, J.***; et al.
ALICE Collaboration

Recent measurements of charm-baryon production in hadronic collisions have questioned the universality of charm--quark fragmentation across different collision systems. In this work the fragmentation of charm quarks into charm baryons is probed, by presenting the first measurement of the longitudinal jet momentum fraction carried by Lambda(+)(c) baryons, z(||)(ch) , in hadronic collisions. The results are obtained in proton-proton (pp) collisions at root s = 13 TeV at the LHC, with Lambda(+)(c) baryons and charged (track-based) jets reconstructed in the transverse momentum intervals of 3 <= p(T)(Lambda c+) < 15 GeV/c and 7 <= p(T)(jet)ch < 15 GeV/c, respectively. The zch k distribution is compared to a measurement of D-0-tagged charged jets in pp collisions as well as to PYTHIA 8 simulations. The data hints that the fragmentation of charm quarks into charm baryons is softer with respect to charm mesons, in the measured kinematic interval, as predicted by hadronization models which include color correlations beyond leading-color in the string formation.

PHYSICAL REVIEW D 109[7], 072005, 2024. DOI: 10.1103/PhysRevD.109.072005

[P185-2024] "Nanowelding of quantum spin-12 chains at minimal dissipation"

Cavalcante, M. F.*; Bonança, M. V. S.*; Miranda, E.*; Deffner, S.

We consider the optimal control of switching on a coupling term between two quantum many-body systems. Specifically, we (i) quantify the energetic cost of establishing a weak junction between two quantum spin-1/2 chains in finite time r and (ii) identify the energetically optimal protocol to realize it. For linear driving protocols, we find that for long times the excess (irreversible) work scales as tau(-n), where n = 1, 2 or a nonuniversal number depending on the phase of the chains. Interestingly, increasing a J(z) anisotropy in the chains suppresses the excess work, thus promoting quasiadiabaticity. The general optimal control problem is solved, employing a Chebyshev Ansatz. We find that the optimal control protocol is intimately sensitive to the chain phases.

PHYSICAL REVIEW B 110[6], 064304, 2024. DOI: 10.1103/PhysRevB.110.064304

[P186-2024] "Negative imaginary potential to model ionization in atoms and molecules by electron impact"

Falkowski, A. G.*; Bettega, M. H. F.; **Lima, M. A. P.***

The low-energy electron-molecule collisions have several implications for the behavior of microscopic and macroscopic environments. One of the most important consequences of this event is molecular ionization due to the electron impact. Since the inclusion of ionization effects through ab initio methods is challenging, we implemented a negative imaginary potential to act as a sinkhole of probability flux to mimic the ionization effects in electron-molecule collisions. We employed an iterative procedure to reproduce the total ionization cross sections computed with the binary-encounter-Bethe model and investigated some Gaussian distributions representing the model potential. Also, in light of obtaining a model with a reasonable physical significance and avoiding arbitrariness, we performed calculations using the probability density as an imaginary potential. Our main goal is to investigate the effect of an absorption potential in the elastic and inelastic channels in ab initio calculations using the Schwinger multichannel method. The results obtained in this study using H2 as a test case are encouraging, since the absorption channel disputes flux probability with other channels.

PHYSICAL REVIEW A 110[2], 022808, 2024. DOI: 10.1103/PhysRevA.110.022808

[P187-2024] "Neutrino trident scattering at the LHC energy regime"

Francener, R.*; Gonçalves, V. P.; **Gratieri, D. R.***

The neutrino trident scattering process in neutrino-tungsten interactions at the LHC energy regime is investigated, and the cross-sections for different leptonic final states in coherent and incoherent interactions are estimated. Furthermore, the associated number of events at FASER nu\documentclass[12pt]{minimal}\usepackage{amsmath}\usepackage{wasysym}\usepackage{amsfonts}\usepackage{amssymb}\usepackage{amsbsy}\usepackage{mathrsfs}\usepackage{upgreek}\setlength{\oddsidemargin}{-69pt}\begin{document}$$\nu $$\end{document}2 detector is estimated considering different predictions for the flux of incident neutrinos on the detector, based on distinct hadronic models for the particle production in pp collisions at ultra-forward rapidities. Our results indicate that the observation of the neutrino trident process is, in principle, feasible at the Forward Physics Facility.

EUROPEAN PHYSICAL JOURNAL C 84[9], 923, 2024. DOI: 10.1140/epjc/s10052-024-13323-2

[P188-2024] "Note on the emission spectrum and trapping states in the Jaynes-Cummings model"

Bertassoli, J. L. T.*; Vidiella-Barranco, A.*

The emission of light from an atom represents a fundamental process that provides valuable insights into the atom- light interaction. The Jaynes-Cummings model is one of the simplest fully quantized models to deal with these interactions, allowing for an analytical solution, while exhibiting notable nontrivial effects. We explore new, to our knowledge, features in the fluorescence emission spectrum for initial "trapping states," which suppress the atomic population inversion. Despite the seemingly dormant activity of the atom, the resulting emission spectra exhibit rich features, and using a dressed-state coordinates formalism, we are able to quantitatively explain the different profiles in the spectrum. We generalize the trapping conditions for nonzero atom-field detuning and also unveil two types of trapping states that lead to spectra with three peaks, in contrast to previously known states: a center peak and one secondary peak on each side. These are a trapping state formed by a Schr & ouml;dinger cat state with Poissonian statistics (Yurke-Stoler state) and also a different type of "perfect trapping state."

JOURNAL OF THE OPTICAL SOCIETY OF AMERICA B-OPTICAL PHYSICS 41[8], c199-c205, 2024. DOI: 10.1364/JOSAB.524429

[P189-2024] "Observation of the J/ψ --- μ+μ-μ+μ- decay in proton-proton collisions at √s=13 TeV"

Hayrapetyan, A.; Tumasyan, A.; Adam, W.; **Chinellato, J. A.***; et al.
CMS Collaboration

The J/psi -> mu(+)mu(-)mu(+)mu(-) decay has been observed with a statistical significance in excess of five standard deviations.

The analysis is based on an event sample of proton-proton collisions at a center-of-mass energy of 13 TeV, collected by the CMS experiment in 2018 and corresponding to an integrated luminosity of 33.6 fb(-1). Normalizing to the J/psi -> mu(+)mu(-) decay mode leads to a branching fraction of [10.1(-2.7)(+3.3)(stat) +/- 0.4(syst)] x 10(-7), a value that is consistent with the standard model prediction.

PHYSICAL REVIEW D 109[11], L111101, 2024. DOI: 10.1103/PhysRevD.109.L111101

[P190-2024] "Paratellurite Nanowires as a Versatile Material for THz Phonon Polaritons"

Mayer, R. A.*; Wehmeier, L.; Torquato, M.; Chen, X. Z.; **Feres, F. H.***; Maia, F. C. B.; Obst, M.; Kaps, F. G.; Luferau, A.; Klopf, J. M.; Corder, S. N. G.; Bechtel, H. A.; González, J. C.; Viana, E. R.; Eng, L. M.; Kehr, S. C.; Freitas, R. O.; Barcelos, I. D.

Polaritons, i.e., hybrid quasi-particles of light and matter resonances, have been extensively investigated due to their potential to enhance light-matter interactions. Although polaritonic applications thrive in the mid-infrared range, their extension to the terahertz (THz) range remains limited. Here, we present paratellurite (alpha-TeO2) nanowires, a versatile material acting as a platform for different types of phonon polaritons. Utilizing synchrotron infrared nanospectroscopy from 10 to 24 THz, we uncover the polaritonic properties of alpha-TeO2 nanowires, showcasing their dual functionality as both a Fabry-P & eacute;rot cavity and a waveguide for surface phonon polaritons. Furthermore, near-field measurements with a free--electron laser as a THz source reveal a localized optical contrast down to 5.5 THz, an indication of hyperbolic bands. Our findings complement the repertoire of polaritonic materials, with significant implications for advancing THz technologies.

ACS PHOTONICS, 2024. DOI: 10.1021/acsphotonics.4c01249 Early Access Date: SEP 2024

[P191-2024] "Photoluminescence and magnetic properties of isostructural europium(III), gadolinium(III) and terbium(III) oxamate-based coordination polymers"

Silveira, C. O. C. da; Oliveira, W. X. C.; Silva Jr., E. N.; Alvarenga, M. E.; Martins, F. T.; Gatto, C. C.; Pinheiro, C. B.; Pedroso, E. F.; Silva, J. P. O.; Marques, L. F.; Santos, M. V.; Torres, F. R.; Euclides, R.; Freire, R. O.; Nunes, W. C.; **Almeida, A. A. de*; Knobel, M.***; Pereira, C. L. M.

Developing and investigating advanced multifunctional materials with magnetic properties as candidates for assembling spin qubits for quantum computing is imperative. A new polytopic ligand based on oxamate and aniline was used to promote the synthesis of three neutral homometallic lanthanide-coordinated polymers. New complexes with the formula {Ln(phox)(3)(DMSO)(2)(H2O)}(n), where Ln = Eu3+ (1), Gd3+ (2), and Tb3+ (3) [phox = N-(phenyl)oxamate and DMSO = dimethylsulfoxide], were synthesized and well characterized by spectroscopic methods as well as X-ray crystallographic analysis. All crystalline structures comprise neutral zigzag chains. The lanthanide ions are linked by three phox ligands, in which two oxygen atoms from two different ligands are responsible for connecting the trivalent lanthanide ions, and one phox ligand completes the coordination sphere in a bis-bidentate mode, together with two DMSO molecules and one water coordination molecule. The coordination sphere of lanthanide ions consisted of spherical capped square antiprism (CSAPR-9) symmetry. The magnetic properties of 1-3 were investigated in the 2-300 K temperature range. The dynamic (ac) magnetic properties of 2 reveal a frequency dependence involving the phonon bottleneck mechanism below 33 K under nonzero applied dc magnetic fields, resulting in an example of a field-induced single-molecule magnet. Solid-state photophysical measurements for Eu3+ (1) and Tb3+ (3) complexes indicate that the N-(phenyl)oxamate ligands are very efficient in sensitizing the lanthanide(iii) ions in the visible region of the electromagnetic spectrum. Compounds 1 and 3 exhibited an emission in the red and green regions, respectively. Experimental results and theoretical calculations using the Sparkle/RM1 method support a quantum efficiency of similar to 72% for 1, suggesting its potential as a candidate for light conversion molecular devices (LCMDs).

DALTON TRANSACTIONS 53[36], 2024. DOI: 10.1039/d4dt01290a

[P192-2024] "Psycho-physio-neurological correlates of qualitative attention, emotion and fl ow experiences in a close--to-real-life extreme sports situation: low- and high-altitude slackline walking"

Barros, M. F. de S.; Stefano, C. A.; **Menezes, L. T. de***; Araújo-Moreira, F. M.; Trevelin, L. C.; Maia, R. P.; Radel, R.; **Castellano, G.***

It has been indicated that extreme sport activities result in a highly rewarding experience, despite also providing fear, stress and anxiety. Studies have related this experience to the concept of flow, a positive feeling that individuals undergo when they are completely immersed in an activity. However, little is known about the exact nature of these experiences, and, there are still no empirical results to characterize the brain dynamics during extreme sport practice. This work aimed at investigating changes in psychological responses while recording physiological (heart rate-HR, and breathing rate-BR) and neural (electroencephalographic-EEG) data of eight volunteers, during outdoors slackline walking in a mountainous environment at two different altitude conditions (1 m-low-walk- and 45 m-high-walk-from the ground). Low-walk showed a higher score on flow scale, while high-walk displayed a higher score in the negative affect aspects, which together point to some level of flow restriction during high-walk. The order of task performance was shown to be relevant for the physiological and neural variables. The brain behavior during flow, mainly considering attention networks, displayed the stimulus-driven ventral attention network-VAN, regionally prevailing (mainly at the frontal lobe), over the goal-directed dorsal attention network-DAN. Therefore, we suggest an interpretation of flow experiences as an opened attention to more changing details in experience', rather than a 'task-focused experience'.

PEERJ 12, e17743, 2024. DOI: 10.7717/peerj.17743

[P193-2024] "Raman scattering spectroscopy of micrometer-sized carbon serpentines"

Zanatta, A. R.; Oliveira Jr, M. H.; **Marques, F. C.***

The stability of carbon-based films is greatly influenced by their intrinsic stress and by the film-substrate interaction that, in certain cases, can induce the formation of micrometer-sized patterns. The study of these patterns (henceforth, C-serpentines) provides important information regarding the mechanical properties of C films and, hence, has motivated several investigations. However, most of these efforts originate from microscope based techniques in which the bond structure details of the C-serpentines are not taken into account. The importance of C-films in practical applications and the absence of Raman spectroscopy studies about C-serpentines form the basis of this paper. Accordingly, this work presents a thorough investigation of a C-film (as deposited by ion-beam deposition) onto the C--serpentine and nearby, as obtained by Raman scattering spectroscopy. Based on the experimental results it is possible to state that, contrary to the C-film (that is made of very small graphite crystallites), the regions occupied by the C-serpentine correspond to larger crystallites (typically >= 100 nm).

Also, the results show that the C-serpentine is less stressed, which is in agreement with its crystallite size as well as with the accepted models that explain the C-serpentine formation.

MATERIALS CHEMISTRY AND PHYSICS 319, 12934, 2024. DOI: 10.1016/j.matchemphys.2024.129343

[P194-2024] "Search for dark matter particles in W+W- events with transverse momentum imbalance in proton--proton collisions at √s=13 TeV"

Hayrapetyan, A.; Tumasyan, A.; Adam, W.; **Chinellato, J. A.***; et al.
CMS Collaboration

A search for dark matter particles is performed using events with a pair of W bosons and large missing transverse momentum. Candidate events are selected by requiring one or two leptons (l = electrons or muons). The analysis is based on proton-proton collision data collected at a center-of-mass energy of 13TeV by the CMS experiment at the LHC and corresponding to an integrated luminosity of 138 fb(-1). No significant excess over the expected standard model background is observed in the l nu qq and 2l2 nu final states of the W+W- boson pair. Limits are set on dark matter production in the context of a simplified dark Higgs model, with a dark Higgs boson mass above the W+W- mass threshold. The dark matter phase space is probed in the mass range 100-300 GeV, extending the scope of previous searches. Current exclusion limits are improved in the range of dark Higgs masses from 160 to 250 GeV, for a dark matter mass of 200 GeV.

JOURNAL OF HIGH ENERGY PHYSICS [3], 134, 2024. DOI: 10.1007/JHEP03(2024)134

[P195-2024] "Search for flavor changing neutral current interactions of the top quark in final states with a photon and additional jets in proton-proton collisions at √s=13 TeV"

Hayrapetyan, A.; Tumasyan, A.; Adam, W.; **Chinellato, J. A.***; et al.
CMS Collaboration

A search for the production of a top quark in association with a photon and additional jets via flavor changing neutral current interactions is presented. The analysis uses proton-proton collision data recorded by the CMS detector at a center-of-mass energy of 13 TeV, corresponding to an integrated luminosity of 138 fb(-1). The search is performed by looking for processes where a single top quark is produced in association with a photon, or a pair of top quarks where one of the top quarks decays into a photon and an up or charm quark. Events with an electron or a muon, a photon, one or more jets, and missing transverse momentum are selected. Multivariate analysis techniques are used to discriminate signal and standard model background processes. No significant deviation is observed over the predicted background. Observed (expected) upper limits are set on the branching fractions of top quark decays: B(t -> u gamma) < 0.95 x 10(-5) (1.20 x 10(-5)) and B(t -> c gamma) < 1.51 x 10(-5) (1.54 x 10(-5)) at 95% confidence level, assuming a single nonzero coupling at a time. The obtained limit for B(t -> u gamma) is similar to the current best limit, while the limit for B(t -> u gamma) is significantly tighter than previous results.

PHYSICAL REVIEW D 109[7], 072004, 2024. DOI: 10.1103/PhysRevD.109.072004

[P196-2024] "Search for long-lived particles using displaced vertices and missing transverse momentum in proton-proton collisions at √s=13 TeV"

Hayrapetyan, A.; Tumasyan, A.; Adam, W.; **Chinellato, J. A.***; et al.
CMS Collaboration

A search for the production of long-lived particles in proton-proton collisions at a center-of-mass energy of 13 TeVat the CERN LHC is presented. The search is based on data collected by the CMS experiment in 2016-2018, corresponding to a total integrated luminosity of 137 fb(-1). This search is designed to be sensitive to long-lived particles with mean proper decay lengths between 0.1 and 1000 mm, whose decay products produce a final state with at least one displaced vertex and missing transverse momentum. A machine learning algorithm, which improves the background rejection power by more than an order of magnitude, is applied to improve the sensitivity. The observation is consistent with the standard model background prediction, and the results are used to constrain split supersymmetry (SUSY) and gaugemediated SUSY breaking models with different gluino mean proper decay lengths and masses. This search is the first CMS search that shows sensitivity to hadronically decaying long-lived particles from signals with mass differences between the gluino and neutralino below 100 GeV. It sets the most stringent limits to date for split-SUSY models and gauge-mediated SUSY breaking models with gluino proper decay length less than 6 mm.

PHYSICAL REVIEW D 109[11], 112005, 2024. DOI: 10.1103/PhysRevD.109.112005

[P197-2024] "Search for W' bosons decaying to a top and a bottom quark in leptonic final states in proton-proton collisions at √s=13 TeV"

Hayrapetyan, A.; Tumasyan, A.; Adam, W.; **Chinellato, J. A.***; et al.
CMS Collaboration

A search for W' bosons decaying to a top and a bottom quark in final states including an electron or a muon is performed with the CMS detector at the LHC. The analyzed data correspond to an integrated luminosity of 138 fb(-1) of proton--proton collisions at a center-of-mass energy of 13TeV. Good agreement with the standard model expectation is observed and no evidence for the existence of the W' boson is found over the mass range examined. The largest observed deviation from the standard model expectation is found for a W' boson mass (m(W)') hypothesis of 3.8TeV with a relative decay width of 1%, with a local (global) significance of 2.6 (2.0) standard deviations. Upper limits on the production cross sections of W' bosons decaying to a top and a bottom quark are set. Left- and right-handed W' bosons with m(W)' below 3.9 and 4.3TeV, respectively, are excluded at the 95% confidence level, under the assumption that the new particle has a narrow decay width. Limits are also set for relative decay widths up to 30%.

JOURNAL OF HIGH ENERGY PHYSICS [5], 046, 2024. DOI: 10.1007/JHEP05(2024)046

[P198-2024] "Soft X-Ray Phase Nanomicroscopy of Micrometer-Thick Magnets"

Neethirajan, J.; Daurer, B. J.; Martinez, M. Di P.; Hrabec, A.; Turnbull, L.; Yamamoto, R.; **Ferreira, M. R.***; Stefancic, A.; Mayoh, D. A.; Balakrishnan, G.; Pei, Z. W.; Xue, P. F.; Chang, L.; Ringe, E.; Harrison, R.; Valencia, S.; Kazemian, M.; Kaulich, B.; Donnelly, C.

Imaging of nanoscale magnetic textures within extended material systems is of critical importance to both fundamental research and technological applications. While high--resolution magnetic imaging of thin nanoscale samples is well established with electron and soft x-ray microscopy,

the extension to micrometer-thick systems currently requires hard x rays, which limits high-resolution imaging to rareearth magnets. Here, we overcome this limitation by establishing soft x-ray magnetic imaging of micrometer-thick systems using the pre-edge phase x-ray magnetic circular dichroism signal, thus making possible the study of a wide range of magnetic materials. By performing dichroic spectroptychography, we demonstrate high spatial resolution imaging of magnetic samples up to 1.7 mu m thick, an order of magnitude higher than conventionally possible with soft x-ray absorption-based techniques. We demonstrate the applicability of the technique by harnessing the pre-edge phase to image thick chiral helimagnets, and naturally occurring magnetite particles, gaining insight into their three-dimensional magnetic configuration. This new regime of magnetic imaging makes possible the study of extended non- rare-earth systems that have until now been inaccessible, including magnetic textures for future spintronic applications, non-rare-earth permanent magnets for energy harvesting, and the magnetic configuration of giant magnetofossils.

PHYSICAL REVIEW X 14[3], 031028, 2024. DOI: 10.1103/PhysRevX.14.031028

[P199-2024] "Structural and Electronic Response of Multigap N-Doped In2Se3: A Prototypical Material for Broad Spectral Optical Devices"

Rodrigues-Fontenele, G.; Fontenele, G.; **Valentim, M. R.***; Freitas, L. V. C.; Rodrigues Junior, G.; Magalhaes Paniago, R.; Malachias, A.

The production of controlled doping in two-dimensional semiconductor materials is a challenging issue when introducing these systems into current and future technology. In some compounds, the coexistence of distinct crystallographic phases for a fixed composition introduces an additional degree of complexity for synthesis, chemical stability, and potential applications. In this work, we demonstrate that a multiphase In2Se3 layered semiconductor system, synthesized with three distinct structures-rhombohedral alpha and beta-In2Se3 and trigonal delta-In2Se3-exhibits chemical stability and well-behaved n--type doping. Scanning tunneling spectroscopy measurements reveal variations in the local electronic density of states among the In2Se3 structures, resulting in a compound system with electronic bandgaps that range from infrared to visible light. These characteristics make the layered In2Se3 system a promising candidate for multigap or broad spectral optical devices, such as detectors and solar cells. The ability to tune the electronic properties of In2Se3 through structural phase manipulation makes it ideal for integration into flexible electronics and the development of heterostructures with other materials.

ACS APPLIED MATERIALS & INTERFACES 16[37], 49902-49912, 2024. DOI: 10.1021/acsami.4c08610, Early Access Date: SEP 2024

[P200-2024] "Subcutaneous adipose tissue radiodensity: An emerging risk factor for severe COVID-19"

Padilha, D. M. H.; Mendes, M. C. S.; **Takahashi, M. E. S.***; Lascala, F.; Silveira, M. N.; Pozzuto, L.; Carrilho, L. A. O.; Guerra, L. D.; Moreira, R. C. L.; Branbilla, S. R.; Ramos, C. D.; Carvalheira, J. B. C.

Background: Adipose tissue radiodensity and metabolic activity may influence COVID-19 outcomes. This study evaluated the association between adipose tissue characteristics and clinical outcomes in COVID-19 patients. Methods: Two retrospective cohorts of hospitalized COVID-19 patients were analyzed. Subcutaneous adipose tissue radiodensity (SATR) and visceral adipose tissue radiodensity were assessed by computed tomography. Fluorine-18-labelled fluorodeoxyglucose PET/computed tomography measured adipose tissue metabolic activity. Associations with mortality, length of stay, ventilation requirement, and complications were examined using regression analyses. Results: High SATR was independently associated with increased mortality risk (OR: 2.70; P = 0.033), longer hospitalization (P < 0.001), higher rates of mechanical ventilation (P = 0.007), and complications: acute kidney injury (P = 0.001), secondary infection (P = 0.007), shock (P = 0.010), and pulmonary embolism (P = 0.011). SATR positively correlated with SAT glucose uptake (r = 0.52) and negatively with leptin levels (r =-0.48). Conclusions: Elevated SATR at COVID-19 diagnosis predicts disease severity and worse outcomes. SATR is a potential prognostic biomarker for acute and chronic inflammatory conditions.

NUTRITION 128, 112561, 2024. DOI: 10.1016/j.nut.2024.112561

[P201-2024] "Superconducting NbC nanoparticles synthesized by laser ablation in a liquid"

Fabris, F.*; García-Flores, A. F.*; Cagigas, J. A. M.; Acuña, J. J. S.; **Rettori, C.*; Urbano, R. R.***

Niobium carbide (NbC) is a high-field type II superconductor with a critical temperature (TC) of 11.1 K, slightly exceeding that of pure Nb (TC = 9 K). The reduction of NbC to the nanoparticle scale leads to significant changes in its critical field and/or the superconducting temperature. This study presents findings on superconducting NbC nanoparticles with TC similar or equal to 10 K produced through laser ablation in acetone, where different conditions of laser fluence and centrifugation were studied. Analysis by X-ray diffraction confirmed the cubic NbC phase, while electron microscopy images displayed approximately 8 nm spherical particles, showing no noticeable size variation with laser fluence. Additionally, magnetization curves exhibited both magnetic and superconducting loops for all investigated samples. A decrease in laser fluence resulted in the suppression of diamagnetic behavior below TC. Furthermore, all samples exhibited a weak electron spin resonance (ESR) Curie-like signal at g similar or equal to 2.0, probably linked to localized defects on the particle's surface. The simultaneous existence of superconductivity and magnetism in nanoparticles has recently garnered significant research attention. This intricate scenario and unique properties arise from the significant enhancement of the surface-to-volume ratio in these superconducting NbC nanoparticles, emphasizing the need for further investigation to unveil novel material properties and shed new light on our comprehension of the superconducting phenomenon in this particular morphology. Superconducting niobium carbide (NbC) nanoparticles produced by laser ablation in acetone at different laser fluences. The magnetic and superconducting properties of the nanoparticles were subsequently studied.

PHYSICAL CHEMISTRY CHEMICAL PHYSICS 26[34], 22706-22714, 2024. DOI: 10.1039/d4cp01481b

[P202-2024] "Systematic study of flow vector fluctuations in √SNN=5.02 TeV Pb-Pb collisions"

Acharya, S.; Adamova, D.; **Chinellato, D. D.*; Guardiano, G. G.*; Liveraro, G. S. S.*; Takahashi, J.***; et al.
ALICE Collaboration

Measurements of the p(T)-dependent flow vector fluctuations in Pb-Pb collisions at root S-NN = 5.02 TeV using azimuthal correlations with the ALICE experiment at the Large Hadron Collider are presented. A four-particle correlation approach [ALICE Collaboration, Phys. Rev. C 107, L051901 (2023)] is used to quantify the effects of flow angle and magnitude fluctuations separately.

This paper extends previous studies to additional centrality intervals and provides measurements of the p(T)-dependent flow vector fluctuations at root S-NN = 5.02 TeV with two--particle correlations. Significant p(T)-dependent fluctuations of the (V) over right arrow (2) flow vector in Pb-Pb collisions are found across different centrality ranges, with the largest fluctuations of up to similar to 15% being present in the 5% most central collisions. In parallel, no evidence of significant p(T)-dependent fluctuations of (V) over right arrow (3) or (V) over right arrow (4) is found. Additionally, evidence of flow angle and magnitude fluctuations is observed with more than 5 sigma significance in central collisions. These observations in Pb-Pb collisions indicate where the classical picture of hydrodynamic modeling with a common symmetry plane breaks down. This has implications for hard probes at high p(T), which might be biased by p(T)-dependent flow angle fluctuations of at least 23% in central collisions. Given the presented results, existing theoretical models should be reexamined to improve our understanding of initial conditions, quark-gluon plasma properties, and the dynamic evolution of the created system.

PHYSICAL REVIEW C 109[6], 065202, 2024. DOI: 10.1103/PhysRevC.109.065202

[P203-2024] "Tau polarization in neutrino-nucleus interactions at the LHC energy range"

Francener, R.*; Gonsalves, V. P.; **Gratieri, D. R.***

Considering that the study of neutrino-nucleus interactions with incident neutrino energy ranges in the GeV-TeV range is feasible at the Large Hadron Collider, we investigate in this paper the degree of polarization P of the (anti)tau lepton produced in (anti)tau neutrino-tungsten interactions. We estimate the differential cross sections and the longitudinal and transverse components of the tau lepton polarization as a function of the tau lepton energy and distinct values of the scattering angle, assuming different values for the energy of the incoming (anti)tau neutrino. Different models for the treatment of the nuclear effects in the parton distribution functions are assumed as input in the calculations. Our results indicate that P < 1 for the neutrino energies reached at the LHC and are almost insensitive to the nuclear effects.

PHYSICAL REVIEW D 109[11], 113005, 2024. DOI: 10.1103/PhysRevD.109.113005

[P204-2024] "Testing hadronic-model predictions of depth of maximum of air-shower profiles and ground-particle signals using hybrid data of the Pierre Auger Observatory"

Halim, A. A.; Abreu, P.; **Aglietta, M.*; Arbeletche, L. Bonneau*; Chinellato, J. A.*; Dobrigkeit, C.*; Fauth, A. C.*; Payeras, A. Machado*; Akim, J. V. Reginatto***; et al.
Pierre Auger Collaboration

We test the predictions of hadronic interaction models regarding the depth of maximum of air-shower profiles, X-max, and ground-particle signals in water-Cherenkov detectors at 1000 m from the shower core, S(1000), using the data from the fluorescence and surface detectors of the Pierre Auger Observatory. The test consists of fitting the measured two-dimensional (S(1000), X-max) distributions using templates for simulated air showers produced with hadronic interaction models Epos-LHC, QGSJet--II-04, SIBYLL 2.3d and leaving the scales of predicted X-max and the signals from hadronic component at ground as free-fit parameters. The method relies on the assumption that the mass composition remains the same at all zenith angles, while the longitudinal shower development and attenuation of ground signal depend on the mass composition in a correlated way. The analysis was applied to 2239 events detected by both the fluorescence and surface detectors of the Pierre Auger Observatory with energies between 10(18.5) eV to 10(19.0) eV and zenith angles below 60 degrees. We found, that within the assumptions of the method, the best description of the data is achieved if the predictions of the hadronic interaction models are shifted to deeper X-max values and larger hadronic signals at all zenith angles. Given the magnitude of the shifts and the data sample size, the statistical significance of the improvement of data description using the modifications considered in the paper is larger than 5 sigma even for any linear combination of experimental systematic uncertainties.

PHYSICAL REVIEW D 109[10], 102001, 2024. DOI: 10.1103/PhysRevD.109.102001

[P205-2024] "The Jaynes-Cummings model: 60 years and still counting"

Larson, J.; Mavrogordatos, T.; Parkins, S.; **Vidiella-Barranco, A.***

2023 marked the 60th anniversary of the Jaynes-Cummings model, a foundational model in quantum optics. Over the years, its importance has expanded beyond traditional light-matter interaction systems, such as cavity QED. This special issue presents a collection of articles that showcase the evolution of the model's applications, blending traditional topics with contemporary developments.

JOURNAL OF THE OPTICAL SOCIETY OF AMERICA B-OPTICAL PHYSICS 41[8], 536847, 2024. DOI: 10.1364/JOSAB.536847

[P206-2024] "The spectrum of radioactive water vapor: the H219O radio-isotopologue"

Voronin, B. A.*; Tennyson, J.; Chesnokova, T. Y.; Chentsov, A. V.; Bykov, A. D.

The absorption spectrum of (H2O)-O-19, a radioactive isotopologue of the water molecule, is predicted using variational nuclear motion calculated based on a high precision potential energy function and ab initio dipole moment surface. Vibrational - rotational energy levels and wave functions, line centers and Einstein coefficients for dipole transitions are calculated. Predicted transition wavenumbers are improved by extrapolating known empirical energy levels of the stable (H2O)-O-16, (H2O)-O-17 and (H2O)-O-18 isotopologues to (H2O)-O-19. A line list for possible atmospheric application is presented which includes air line broadening coefficients. The calculations span a wide spectral range covering infrared and visible wavelengths, and are appropriate for temperatures up to 1000 K. Windows suitable for observing absorption by (H2O)-O-19 are identified and comparisons made with the infrared spectra of water vapor in natural abundance, (H2O)-O-15 and (H2O)-O-14.

JOURNAL OF RADIOANALYTICAL AND NUCLEAR CHEMISTRY, 2024. DOI: 10.1007/s10967-024-09677-2, Early Access Date: SEP 2024

[P207-2024] "Third order interactions shift the critical coupling in multidimensional Kuramoto models"

Fariello, R.; **Aguiar, M. A. M. de***

The study of higher order interactions in the dynamics of Kuramoto oscillators has been a topic of intense research. Previous works have demonstrated that such interactions can give rise to interesting new phenomena such as multi-stability and synchronization even if the interaction between oscillators is repulsive.

Here we consider higher order interactions in the multidimensional Kuramoto model where pairs (1-simplex), triplets (2-simplex) and quadruples (3-simplex) of oscillators interact simultaneously with different coupling strengths, k(1), k(2) and k(3), respectively. For the types of asymmetric interactions considered, we show that three body terms shift the critical coupling for synchronization towards higher values, except in 2 dimensions where a cancellation occurs. However, after the transition, three and four body interactions combine to facilitate synchronization. We also show that, for fixed values of k(2) and k(3), and fully connected networks, the behavior of the order parameter r(k(1)) is described by a universal curve given by its value at k(2) = k(3) = 0, shifted along the k(1) axis. Similar to the 2-dimensional case with asymmetric interactions, bi-stability and hysteresis develop for large enough higher order interactions. Multi-stability, typical of symmetric higher order interactions, is not found. We show simulations in three and four dimensions to illustrate the dynamics.

CHAOS SOLITONS & FRACTALS 187, 115467, 2024. DOI: 10.1016/j.chaos.2024.115467

[P208-2024] "TPDH-Graphene as a New Anodic Material for Lithium Ion Battery: DFT-Based Investigations"

Quispe, J. G.; Ipaves, B.; **Galvao, D. S.***; Autreto, P. A. da S.

The potential of tetra-penta-deca-hexagonal graphene (TPDH--gr), a recently proposed 2D carbon allotrope as an anodic material in lithium ion batteries (LIBs), was investigated through density functional theory calculations. The results indicate that Li-atom adsorption is moderate (around 0.70 eV), allowing for easy desorption. Moreover, energy barriers (0.08-0.20 eV), diffusion coefficient (>6 x 10(-6) cm(2)/s), and open circuit voltage (0.29 V) calculations show rapid Li atom diffusion on the TPDH-gr surface, stable intercalation of lithium atoms, and good performance during the charge and discharge cycles of the LIB. These findings, combined with the intrinsic metallic nature of TPDH-gr, indicate that this new 2D carbon allotrope is a promising candidate for use as an anodic LIB material.

ACS OMEGA, 2024. DOI: 10.1021/acsomega.4c06252, Early Access Date: SEP 2024

[P209-2024] "Trade-off relations between Bell nonlocality and local Kochen-Specker contextuality in generalized Bell scenarios"

Porto, L. E. A.*; Ruffolo, G.*; Rabelo, R.*; Cunha, M. T.; Kurzynski, P.

The relations between Bell nonlocality and Kochen-Specker contextuality have been subject of research from many different perspectives in the last decades. Recently, some interesting results on these relations have been explored in the so--called generalized Bell scenarios, that is, scenarios where Bell spatial separation (or agency independence) coexist with (at least one of the) parties' ability to perform compatible measurements at each round of the experiment. When this party has an n-cycle compatiblity setup, it was first claimed that Bell nonlocality could not be concomitantly observed with contextuality at this party's local experiment. However, by a more natural reading of the definition of locality, it turns out that both Bell nonlocality and local contextuality can, in fact, be jointly present. In spite of it, in this work we prove that in the simplest of those scenarios there cannot be arbitrary amounts of both of these two resources together. That is, in these cases we show that the violation of any Bell inequality limits the possible violations of any local noncontextuality inequality. We also explore this trade-off relation using quantifiers of nonlocality and contextuality, discussing how such a relation can be understood in terms of a 'global' notion of contextuality, and we study possible extensions of this result to other scenarios.

NEW JOURNAL OF PHYSICS 26[8], 083028, 2024. DOI: 10.1088/1367-2630/ad7167

[P210-2024] "Transforming Two-Dimensional Carbon Allotropes into Three-Dimensional Ones through Topological Mapping: The Case of Biphenylene Carbon (Graphenylene)"

T**romer, R. M.*; Felix, L. C.***; Baughmann, R. H.; **Galvao, D. S.***; Woellner, C. F.

In this work, we propose a new methodology for obtaining three-dimensional (3D) carbon allotrope structures from 2D ones through topological mapping. The idea is to select a 3D target structure and "slice" it along different structural directions, creating a series of 2D structures. As a proof of concept, we chose the tubulane structure 12-hexa(3,3) as a target. Tubulanes are 3D carbon allotropes based on cross-linked carbon nanotubes. One of the obtained 2D "sliced" structures was mapped into the biphenylene carbon (BPC). We showed that compressing BPC in-plane, biaxially, followed by compression along the z direction using different strain rates could generate not only the target tubulane 12-hexa(3,3) structure but also at least two others: bcc-C6 and an unreported member of the tubulane family, which we called tubulane X. The methodology proposed here is entirely general; it can be used coupled with any quantum method. Considering that the 2D biphenylene carbon network, which is closely related to BPC, has been recently synthesized, the approach proposed here opens new perspectives to obtain new 3D carbon allotropes from 2D structures.

JOURNAL OF PHYSICAL CHEMISTRY A 128[35], 7346-7352, 2024. DOI: 10.1021/acs.jpca.4c01339

[P211-2024] "Tuning the electronic and optical properties of two-dimensional diboron-porphyrin by strain engineering: A density functional theory investigation"

Felix, I. M.*; Andrade, F. M.*; Woellner, C. F.*; Galvao, D. S.*; Tromer, R. M.*

We used DFT simulations to study the electronic and optical properties of a 2D crystal called 2D DiboronPorphyrin (2DDP). Our results show that strain can tune 2DDP's electronic properties from semiconducting to metallic, depending on strain direction. The unstrained system has a 0.6 eV band gap, which increases with strain perpendicular to the B-B bond, while parallel strain induces metallic behavior. Additionally, 2DDP's optical activity spans from infrared to ultraviolet and can be strain-tuned, highlighting its potential for electro-opto-mechanical applications.

CHEMICAL PHYSICS LETTERS 856, 141604, 2024. DOI: 10.1016/j.cplett.2024.141604

[P212-2024] "Ultrathin natural biotite crystals as a dielectric layer for van der Waals heterostructure applications"

Oliveira, R. de; **Yoshida, A. B. B.***; Rabahi, C. R.; Freitas, R.; Teixeira, V. C.; Matos, C. J. S. de; Gobato, Y. G.; Barcelos, I. D.; Cadore, A. R.

Biotite, an iron-rich mineral belonging to the trioctahedral mica group, is a naturally abundant layered material (LM) exhibiting attractive electronic properties for application in nanodevices. Biotite stands out as a non-degradable LM under ambient conditions, featuring high-quality basal cleavage-a significant advantage for van der Waals heterostructure (vdWH) applications. In this work, we present the micro-mechanical exfoliation of biotite down to monolayers (1Ls),

yielding ultrathin flakes with large areas and atomically flat surfaces. To identify and characterize the mineral, we conducted a multi-elemental analysis of biotite using energy-dispersive spectroscopy mapping. Additionally, synchrotron x-ray fluorescence and infrared nano-spectroscopy were employed to probe its iron content and vibrational signature in few-layer form, respectively, with sensitivity to the layer number. We have also observed good morphological and structural stability in time (up to 12 months) and no important changes in their physical properties after thermal annealing processes in ultrathin biotite flakes. Conductive atomic force microscopy evaluated its electrical capacity, revealing an electrical breakdown strength of approximately 1 V nm-1. Finally, we explore the use of biotite as a substrate and encapsulating LM in vdWH applications. We have performed optical and magneto-optical measurements at low temperatures. We find that ultrathin biotite flakes work as a good substrate for 1L-MoSe2, comparable to hexagonal boron nitride flakes, but it induces a small change of the 1L-MoSe2 g-factor values, most likely due to natural impurities on its crystal structure. Furthermore, our results show that biotite flakes are useful systems to protect sensitive LMs such as black phosphorus from degradation for up to 60 days in ambient air. Our study introduces biotite as a promising, cost-effective LM for the advancement of future ultrathin nanotechnologies.

NANOTECHNOLOGY 35[50], 505703, 2024. DOI: 10.1088/1361-6528/ad7b3a

[P213-2024] "X-ray spectroscopic investigation of crystal fields in Ce2Rh1-xIrxIn8 heavy fermions"

Christovam, D. S.; Marino, A.; Falke, J.; Liu, C. E.; Chang, C. F.; Kuo, C. Y.; Stockert, O.; Wirth, S.; Haverkort, M. W.; Zwicknagl, G.; Severing, A.; Rosa, P. F. S.; **Caffer, A. M.*; Carvalho, M. H.*; Pagliuso, P. G.***

The higher dimensionality in the crystal fields of the Ce2MIn8 (M = Rh, Ir) compounds and its interplay with hybridization and disorder are key ingredients to understand the complex phase diagrams by this family, which have been explored extensively by macroscopic techniques. Here, we present an investigation of the crystalelectric field schemes of Ce2Rh1-xIrxIn8 using x-ray absorption spectroscopy. Our full multiplet calculations for the 4f(1) configuration of Ce3+ to describe the temperature-dependent linear dichroism in Ce2MIn8 are consistent with a Gamma(1)(7) = root/1 - alpha(2) center dot vertical bar -/+ 3/2 > - vertical bar center dot vertical bar +/- 5/2 > ground state containing a predominant d +/- 3/2) contribution that increases further with x. This enhancement is believed to favor superconductivity in Ce-based heavy fermion materials, observed in previous results in the CeMIn5 family. Our recent observations shed light on the unexpected emergence of the ambient-pressure superconducting dome in the center of the composition phase diagram and its subsequent suppression on the Ir-rich side due to the early onset of fluctuations associated with the structurally more disordered state, inferred from previous neutron magnetic diffraction experiments.

PHYSICAL REVIEW B 110[7], 075161, 2024. DOI: 10.1103/PhysRevB.110.075161

***Autores da comunidade IFGW**
Fonte: Web of Science on-line (WOS)

Eventos publicados

[P214-2024] "Data handling of CYGNO experiment using INFN-Cloud solution"

Amaro, F. D.; Antonacci, M.; Antonietti, R.; **Kemp, E.***; et al.
Espinal X.; DeVita R.; Laycock P.; Shadura O. (Ed.)

The INFN Cloud project was launched at the beginning of 2020, aiming to build a distributed Cloud infrastructure and provide advanced services for the INFN scientific communities. A Platform as a Service (PaaS) was created inside INFN Cloud that allows the experiments to develop and access resources as a Software as a Service (SaaS), and CYGNO is the beta-tester of this system. The aim of the CYGNO experiment is to realize a large gaseous Time Projection Chamber based on the optical readout of the photons produced in the avalanche multiplication of ionization electrons in a GEM stack. To this extent, CYGNO exploits the progress in commercial scientific Active Pixel Sensors based on Scientific CMOS for Dark Matter search and Solar Neutrino studies. CYGNO, like many other astroparticle experiments, requires a computing model to acquire, store, simulate and analyze data typically far from High Energy Physics (HEP) experiments. Indeed, astroparticle experiments are typically characterized by being less demanding of computing resources with respect to HEP ones but have to deal with unique and unrepeatable data, sometimes collected in extreme conditions, with extensive use of templates and montecarlo, and are often re-calibrated and reconstructed many times for a given data set. Moreover, the varieties and the scale of computing models and requirements are extremely large. In this scenario, the Cloud infrastructure with standardized and optimized services offered to the scientific community could be a useful solution able to match the requirements of many small/medium size experiments. In this work, we will present the CYGNO computing model based on the INFN cloud infrastructure where the experiment software, easily extendible to similar experiments to similar applications on other similar experiments, provides tools as a service to store, archive, analyze, and simulate data.

26th INTERNATIONAL CONFERENCE ON COMPUTING IN HIGH ENERGY AND NUCLEAR PHYSICS, CHEP, 2023.

EPJ Web of Conferences 295, 07013, 2024 DOI: 10.1051/epjconf/202429507013

[P215-2024] "Developing Microstructured Polymer Optical Fibers for Sensing Applications"

Souza, E. A. V.*; Cordeiro, C. M. B.*

This study discusses microstructured polymer optical fiber manufacturing, focusing on capillary fibers and their transformation into bottle resonators through post-processing. Our study highlights the simplicity and cost-effectiveness of the experimental setup utilized for capillary fabrication, facilitating streamlined in-line production processes.

LATIN AMERICAN WORKSHOP ON OPTICAL FIBER SENSORS, LAWOFS, 2024.
IEEE

[P216-2024] "Exploring the Theoretical Landscape of BehCreative: Artistic and Therapeutic Possibilities of an Extended Digital Musical Instrument"

Partesotti, E.; **Castellano, G.***; Manzolli, J.
Brooks A. L. (Ed.)

In the digital age, technology has become ubiquitous in various fields of knowledge, functioning as an extension of the human body - akin to a technological body. Consequently, it acquires ecological validity in our daily lives and offers a path for developing studies rooted in Embodied Cognition. This idea is illustrated by BehCreative, an Extended Digital Musical Instrument (EDMI) introduced and presented in this article. The article delineates the design, mapping and architecture of BehCreative from both musical and cognitive standpoints.

Moreover, it explores how these instruments bridge the divide between traditional musical interfaces and immersive technologies, thereby redefining the limits of artistic expression and therapeutic interventions. The article highlights that BehCreative, as a hybrid instrument, holds the potential to facilitate therapeutic recovery and serve as an artistic tool for expressive purposes. Given its hybrid nature, BehCreative presents diverse possibilities for exploring users' behavioral learning, as evidenced by the results of a mentioned exploratory study. Consequently, it substantiates the hypothesis of being an instrument that warrants examination from an interdisciplinary perspective.

ARTSIT, INTERACTIVITY AND GAME CREATION, PT 1, ARTSIT, 2023.

Lecture Notes of the Institute for Computer Sciences Social Informatics and Telecommunications Engineering 564, 3-15, 2024. DOI: 10.1007/978-3-031-55319-6_1

[P217-2024] "Hollow-core fiber-based sensors: recent advancements in Brazil"

Osorio, J. H.; **Cordeiro, C. M. B.***

We report on our recent investigations carried out in Brazil focusing on the application of hollow-core photonic crystal fibers as platforms for new optical sensors. Herein, we discuss the potentialities of using hollow-core fibers for monitoring parameters such as curvature, temperature, and displacement. Our results contribute to enlarging the framework of hollow--core fiber applications and the impact of this family of optical fibers in the next developments in sensing technologies.

LATIN AMERICAN WORKSHOP ON OPTICAL FIBER SENSORS, LAWOFS, 2024.
IEEE

[P218-2024] "Influence of Delays in Functional Connectivity to Distinguish Motor Imagery Tasks"

Vazquez, P. F. G. de*; Stefano Filho, C. A.*; Castellano, G.*
Salas J. A. R.; Cota V. R.; Villota H.; Vasquez D. B. (Ed.)

Motor imagery is a cognitive technique wherein individuals mentally rehearse bodily movements. Recognized for its alignment with various cognitive and motor functions, motor imagery has become pivotal in brain computer interface applications, especially for motor rehabilitation and neuroprosthetics. Using electroencephalography, a preferred modality for its portability and high temporal precision, our study sought to address the variability challenges in electroencephalography signals, often a bottleneck in brain computer interfaces efficacy. We delved into the role of delay occurrences in shaping the maximal functional connectivity within motor imagery electroencephalography tasks obtained with the motifs' synchronization method. Preliminary findings suggest that specific delay occurrences may play a crucial role in functional connectivity, holding implications for future brain computer interfaces applications and motor rehabilitation protocols.

COMPUTATIONAL NEUROSCIENCE, LAWCN, 2023

[P219-2024] "Laboratory test of a perimeter monitoring system based on optical fiber interferometer"

Cardoso, F. H.; Penze, R. S.; Barros, L. P.; Rosolem, J. B.; Bassan, F. R.; Diago, V.; Neves, F. S.; Ribeiro, A. de A.; **Pirota, K. R.***

This article describes the results of laboratory tests of the perimeter monitoring system, which is based on optical interferometry according to the Dual-Michelson principle. The tests were carried out in a controlled laboratory environment. The article presents the results obtained and shows a way to effectively implement the system. The results show that the system has the potential to improve safety and monitoring and provide valuable results in the laboratory that can later be applied in a real environment.

LATIN AMERICAN WORKSHOP ON OPTICAL FIBER SENSORS, LAWOFS 2024. IEEE

[P220-2024] "Motion Constraints and Control of the UR5e Robot Based on Its Redundancy"

Terreros, R.; Morales, S.; Céspedes, A.; **Fabian, J.*;** Canahuire, R.

This article explores the utilization of manipulator redundancy, focusing on motion constraints and control applications for the UR5e robotic arm. The study investigates the kinematic redundancy inherent in the UR5e and its implications for enhancing adaptability and optimizing performance. Various control strategies, including joint limits, manipulability constraints, and obstacle avoidance, are examined to showcase the versatility of redundancy utilization. The UR5e's response to obstacles and restricted movements is analyzed, highlighting the system's robustness in achieving desired end--effector positions. Through a comprehensive exploration of redundancy in the UR5e manipulator, this research contributes valuable insights into optimizing robotic performance and adaptability in complex and dynamic environments.

9th INTERNATIONAL CONFERENCE ON CONTROL AND ROBOTICS ENGINEERING, ICCRE, 2024.

International Conference on Control and Robotics Engineering, IEEE, 162-167, 2024. DOI: 10.1109/ICCRE61448.2024.10589799

[P221-2024] "Nonlinear-optical material developments since 2000: characterization, data tables, and best practices"

Vermeulen, N.; Espinosa, D.; Ball, A.; **Padilha, L.*;** et al.
Dudley J. M.; Peacock A. C.; Stiller B.; Tissoni G. (Ed.)

The field of nonlinear optics (NLO) has been continuously growing over the past decades, and several NLO data tables were published before the turn of the century. After the year 2000, there have been major advances in materials science and technology beneficial for NLO research, but a data table providing an overview of the post-2000 developments in NLO has so far been lacking. Here, we introduce a new set of NLO data tables listing a representative collection of experimental works published since 2000 for bulk materials, solvents, 0D-1D-2D materials, metamaterials, fiber waveguiding materials, on-chip waveguiding materials, hybrid waveguiding systems, and THz NLO materials. In addition, we provide a list of best practices for characterizing NLO materials. The presented data tables and best practices form the foundation for a more adequate comparison, interpretation, and practical use of already published NLO parameters and those that will be published in the future.

NONLINEAR OPTICS AND ITS APPLICATIONS, 2024.

Proceedings of SPIE 13004, 130040F, 2024. DOI: 10.1117/12.3022590

[P222-2024] "Preliminary Findings from BehCreative: Exploring the Potential of Extended Digital Music Instruments for Music Therapy and Rehabilitation"

Partesotti, E.; **Castellano, G.***; Manzolli, J.
Brooks A. L. (Ed.)

The usefulness of traditional musical instruments has already been demonstrated in music therapy and rehabilitation. In recent years, virtual reality systems have also been shown to promote good cognitive and motor rehabilitation results. Nevertheless, there are still few studies joining these things. The aim of this study was to demonstrate the application potential of an Extended Digital Musical Instrument (EDMI), BehCreative, in those areas, focusing on its ability to promote engagement, motivation, and confidence among users. For this, Gibson's concept of affordance to study users' creative behavior was used. Three healthy subjects participated in this study. Virtual Affordances (VAs) used by users during an exploratory phase and their Motion Development (jerk) were measured, and they answered the Affective Sliders self-assessment questionnaire. The results indicate a positive impact of BehCreative on emotional reactions, physical activities, and creative learning, opening avenues for future research and practical applications in the fields of motor learning and human-computer interaction in music therapy and rehabilitation.

ARTSIT, INTERACTIVITY AND GAME CREATION, PT 1, ARTSIT, 2023.

Lecture Notes of the Institute for Computer Sciences Social Informatics and Telecommunications Engineering 564, 27-40, 2024. DOI: 10.1007/978-3-031-55319-6_3

[P223-2024] "Salt-Doped Agar-Based Optical Fibers for Electric Current Sensing"

Rosa, L. O.; **Cordeiro, C. M. B.***; Fujiwara, E.

This work reports an agar-made, biodegradable optical fiber for electric current measurements. The agar's mineral impurities sustain the charges' flow through the fiber structure, causing refractive index modulation by thermo-optic effect. Moreover, doping the agar solution with NaCl improves the electrical conductivity and sensitivity. We interrogate the sensor response by specklegram analysis, yielding a time-constant reduction in the decaying correlation coefficient curves as the current magnitude increases. Furthermore, oscillations in the speckle pattern manifest for exceeding currents, possibly due to the formation of a dielectric layer within the fiber structure.

LATIN AMERICAN WORKSHOP ON OPTICAL FIBER SENSORS, LAWOFS, 2024.
IEEE

[P224-2024] "Studying Lensed Optical Fiber Tips for Vibrometer Applications"

Morais, E. F.*; Cordeiro, C. M. B.*

Lensed optical fiber tips are widely used in fiber sensing applications. The fabrication process of these lenses allows for precise control over parameters such as working distance, beam waist radius at the focus, and reflectivity at the tip. This control enables the measurement of the frequency of vibration of a vibrating mirror, showcasing the versatility and effectiveness of these lenses in optical fiber sensing.

LATIN AMERICAN WORKSHOP ON OPTICAL FIBER SENSORS, LAWOFS, 2024.
IEEE

[P225-2024] "Studying New-Generation Hollow-Core Fibers for Acousto-Optic Sensors"

Silva, R. E. da*; Osório, J. H.; Benabid, F.; Webb, D. J.; Gérôme, F.; Franco, M. A. R.; **Cordeiro, C. M. B.***

We demonstrate highly efficient modulation of a tubular lattice hollow core fiber by means of flexural acoustic waves. The acousto-optic parameters required for fluid sensing are numerically and experimentally investigated. The results point out high sensor's sensitivity to characterize fluid properties, such as refractive index, density, and viscosity.

LATIN AMERICAN WORKSHOP ON OPTICAL FIBER SENSORS, LAWOFS 2024.
IEEE

[P226-2024] "The Influence of PVTf on Machine Learning Estimation of IGBT Junction Temperature"

Ribeiro, A.; Carvalho, R.; Silva, P. da; Lima, G.; Prym, G.; Barros, T.; **Marques, F.***; Villalva, M.
Bendaoud M.; ElFathi A.; Bakhsh F. I.; Pierluigi S. (Ed.)

The literature indicates that the PV inverter is the element of a photovoltaic plant most prone to failure. For this reason, power electronics converters are generally responsible for most photovoltaic projects' operating and maintenance costs. This article describes the influence of PVTf (power, voltage, ambient temperature, and frequency) on the IGBT junction temperature. We use correlation coefficients and machine learning techniques on the dataset in (Tomislav et al. in IEEE Transactions on Power Electronics 34:7161-7171, 2019). We perform feature selection and the impacts of removing one or more inputs on model training. Data analysis indicates that input power is the most important attribute in the studied dataset and decision tree model presented the best results for the regression problem when compared with MLP and linear regressor. The tool took good advantage of the most important features at the beginning and only considered the less important ones for fine-tuning in the most distant nodes.

ADVANCES IN CONTROL POWER SYSTEMS AND EMERGING TECHNOLOGIES, VOL 2, ICESA, 2023.

Advances in Science Technology and Innovation, 107-116, 2024. DOI: 10.1007/978-3-031-51796-9_13

Material editorial

[M001-2024] "Women in Nano Editorial"

Conrad, J. C.; **Cotta, M. A.***; Tamada, K.; Grace, A. N.
Editorial Material

ACS APPLIED NANO MATERIALS 7[16], 18089-18093, 2024. DOI: 10.1021/acsanm.4c04215

Correção

[Co001-2024] "Prediction of DNA rejoining kinetics and cell survival after proton irradiation for V79 cells using Geant4--DNA (vol 105, 102508, 2023)"

Sakata, D.; Hirayama, R.; Shin, W. G.; **Bernal, M. A.*;** et al.
Correction

PHYSICA MEDICA-EUROPEAN JOURNAL OF MEDICAL PHYSICS 124, 103375, 2024. DOI: 10.1016/j.ejmp.2024.103375

***Autores da comunidade IFGW**
Fonte: Web of Science on-line (WOS)

Defesas de Dissertações do IFGW

[D020-2024] "Modulador acusto-óptico atuado piezoeletricamente em plataformas de Nitreto de Aluminio(AlN)"
Aluno: Pedro Ariston Costa Pessoa
Orientador: Prof. Dr. Gustavo Silva Wiederhecker
Data: 16/09/2024

[D021-2024] "Caracterização de Detector de Pixel Híbrido Baseado em Medipix3RX"
Aluno: Letícia Braga da Rosa
Orientador: Profa. Dra. Alessandra Tomal
Data: 17/09/2024

[D022-2024] "Ressonância Paramagnética Eletrônica de Spins Localizados em Candidatos A Isolantes Topológicos"
Aluno: Gabriel Aller Tolentino Oliveira
Orientador: Prof. Dr. Eduardo Miranda
Data: 20/09/2024

[D023-2024] "Desenvolvimento de Junções Josephson e Caracterização de Qubits Supercondutores Transmon em Cavidades 3D Utilizando Litografia de Feixe de Elétrons de Baixa Energia"
Aluno: Gustavo Moreto Pimenta
Orientador: Prof. Dr. Francisco Paulo Marques Rouxinol
Data: 23/09/2024

[D024-2024] "Condições iniciais em colisões de íons pesados relativísticos e a estrutura 3D do próton"
Aluno: Gabriel Rabelo Soares
Orientador: Prof. Dr. Jun Takahashi
Data: 10/10/2024

[D025-2024] "Estrutura não-perturbativa do vértice quark-glúon projetado transversalmente"
Aluno: Gustavo Linhares Teixeira
Orientador: Profa. Dra. Arlene Cristina Aguilar
Data: 18/10/2024

[D026-2024] "Tremor characterization based on wearable sensors"
Aluno: Caetano Ternes Coimbra
Orientador: Prof. Dr. Rickson Coelho Mesquita
Data: 30/10/2024

Defesas de Teses do IFGW

[T013-2024] "Dissipação em Sistemas Optomecânicos: de Forças Ópticas a Redes Quânticas"
Aluno: André Garcia Primo
Orientador: Prof. Dr. Thiago Pedro Mayer Alegre
Data: 18/09/2024

[T014-2024] "Convergência do acoplamento multicanal no espalhamento de elétrons de baixa energia por moléculas: aplicações do método multicanal de Schwinger"
Aluno: Alan Guilherme Falkowski
Orientador: Prof. Dr. Marco Aurélio Pinheiro Lima
Data: 10/10/2024

[T015-2024] "Estudo das Propriedades Estruturais de Nanossistemas por Difração Elétrons com Precessão (PED)"
Aluno: Leonardo Marcon Corrêa
Orientador: Prof. Dr. Daniel Mário Ugarte
Data: 11/10/2024

[T016-2024] "Engineering One- and Two-Dimensional Supramolecular Porous Planar Carbon Lattices"
Aluno: Alisson Ceccatto dos Santos
Orientador: Prof. Dr. Abner de Siervo
Data: 29/11/2024

Fonte: Portal IFGW/Eventos
Disponível em: https://portal.ifi.unicamp.br/a-instituicao/eventos/month.calendar/2023/12/14/-

Defesas de Dissertações e Teses do PECIM

***Sem atualização na página no período**

Fonte: Página do PECIM
Disponível em: https://www.pecim.unicamp.br/bancas

Abstracta

Instituto de Física
Diretor: Profa. Dra. Mônica Alonso Cotta
Diretora Associada: Prof. Dr. Marcos Cesar de Oliveira
Universidade Estadual de Campinas - UNICAMP
Cidade Universitária Zeferino Vaz
13083-859 - Campinas - SP - Brasil
e-mail: secdir@ifi.unicamp.br
Fone: +55 19 3521-5300

Publicação

Biblioteca do Instituto de Física Gleb Wataghin
http://portal.ifi.unicamp.br/biblioteca
Instagram: @bif.unicamp

Diretora Técnica: Sandra Maria Carlos Cartaxo
Coordenadora da Comissão de Biblioteca: Profa. Dra. Arlene Cristina Aguilar

Elaboração e editoração:
Maria Graciele Trevisan (Bibliotecária)
Artes gráficas: Júlia da Silva Oliveira (Estagiária)
Contato: infobif@ifi.unicamp.br